The Journal of Undergraduate Research in Physics

CONTENTS

Volume 12, Number 1
November, 1993

Published by the Physics Department of Guilford College
for
The American Institute of Physics and the Society of Physics Students

THE JOURNAL OF UNDERGRADUATE RESEARCH IN PHYSICS

This journal is devoted to research work done by undergraduate students in physics and its related fields. It is to be a vehicle for the exchange of ideas and information by undergraduate students. Information for students wishing to submit manuscripts for possible inclusion in the Journal follows.

ELIGIBILITY
The author(s) must have performed all work reported in the paper as an undergraduate student(s). The subject matter of the paper is open to any area of pure or applied physics or physics related field.

SPONSORSHIP
Each paper must be sponsored by a full-time faculty member of the department in which the research was done. A letter from the sponsor, certifying that the work was done by the author as an undergraduate and that the sponsor is willing to be acknowledged at the end of the paper, must accompany the manuscript if it is to be considered for publication.

SUBMISSION
Two copies of the manuscript, the letter from the sponsor and a telephone number or E-Mail address where the author can be reached should be sent to:

Dr. Rexford E. Adelberger, Editor
THE JOURNAL OF UNDERGRADUATE
RESEARCH IN PHYSICS
Physics Department
Guilford College
Greensboro, NC 27410

FORM
The manuscript should be typed, double spaced, on 8 1/2 x 11 inch sheets. Margins of about 1.5 inches should be left on the top, sides, and bottom of each page. Papers should be limited to fifteen pages of text in addition to an abstract (not to exceed 250 words) and appropriate drawings, pictures, and tables.

Manuscripts may be submitted on a disk that can be read by a MacIntosh™. The files must be compatible with MacWrite™, MicroSoft Word™ , PageMaker™ or WordPerfect™.

ILLUSTRATIONS
Line drawings should be made with black ink on plain white paper. Each figure or table must be on a separate sheet. Photographs must have a high gloss finish. If the submission is on a disk, the illustrations should be in PICT, TIFF or EPS format.

CAPTIONS
A brief caption should be provided for each illustration or table, but it should not be part of the figure. The captions should be listed together at the end of the manuscript

EQUATIONS
Equations should appear on separate lines, and may be written in black ink. We use EXPRESSIONIST™ to format equations in the Journal.

FOOTNOTES
Footnotes should be typed, double spaced and grouped together in sequence at the end of the manuscript.

PREPARING A MANUSCRIPT
A more detailed set of instructions for authors wishing to prepare manuscripts for publication in the Journal of Undergraduate Research in Physics can be found in Volume 8 #1 which appeared in October of 1989 or in Volume 11 #2 which appeared in May of 1993.

SUBSCRIPTION INFORMATION

The Journal is published twice each academic year, issue # 1 appearing in November and issue # 2 in May of the next year. There are two issues per volume.

TYPE OF SUBSCRIBER	PRICE PER VOLUME
Individual	$US 5.00
Institution	$US 10.00

Foreign subscribers add $US 2.00 for surface postage, $US 10.00 for air freight.

Back issues may be purchased by sending $US 15.00 per volume to the editorial office.

To receive a subscription, send your name, address, and check made out to **The Journal of Undergraduate Research in Physics (JURP)** to the editorial office:

JURP
Physics Department
Guilford College
Greensboro, NC 27410

The Journal of Undergraduate Research in Physics is sent to each member of the Society of Physics Students as part of their annual dues.

VOLUME 12
ACADEMIC YEAR 1993-1994

The Journal of Undergraduate Research in Physics

ISSN 0731 - 3764

Published by the Physics Department
of Guilford College
for
The American Institute of Physics
and
The Society of Physics Students

THERMAL CONDUCTIVITY OF HIGH T_C SUPERCONDUCTING CERAMICS

James S. Middleton *
Department of Physics
Miami University
Oxford, OH 45056
received June 2, 1992

ABSTRACT

We made measurements of the thermal conductivity of two high T_c Superconducting ceramics. Our $Y_1Ba_2Cu_3O_{7-x}$ results confirm one of two previously conflicting measurements which differed in magnitude by a factor of six. Our agreement with the larger thermal conductivity values is likely due to sample chemical phase purity. Our data on $Bi_2CaSr_2Cu_2O_{9-x}$ confirms a previous measurement and substantiates our experimental technique. A discussion of theory related to thermal conductivity of these substances is included.

INTRODUCTION

Soon after the discovery of the $Y_1Ba_2Cu_3O_{7-x}$ superconductor, many measurements of its various properties were made, including two independent measurements of the thermal conductivity. [1,2] While the qualitative features of the two thermal conductivity vs. temperature [κ vs. T] results were the same, they differed by a factor of six in magnitude. To clarify this discrepancy, we measured the thermal conductivity of a commercially produced sample of this material. The thermal conductivity (κ) is defined by Fourier's law:

$$\kappa = \frac{\frac{dQ}{dt}\Delta x}{A\ \Delta T}\ , \qquad (1)$$

where dQ/dt is the rate of heat flow through cross sectional area A over a distance Δx with a temperature gradient ΔT. The kinetic theory of gases predicts a value for the thermal conductivity:

$$\kappa = \frac{1}{3} C_v v l\ , \qquad (2)$$

where C_v is the specific heat, v is the carrier group velocity and l is the carrier mean free path between scattering centers.

The thermal conductivity of these materials is dominated by phonons, quanta of energy carried by lattice vibrations. In the non-superconducting state, the heat transfer is limited by the scattering of these phonons. A primary mechanism for such scattering is the electron-phonon interaction. Below T_c, the critical temperature, the electrons become bound into Cooper pairs, resulting in the vanishing of electrical resistance. This implies a reduced ability of the electrons to scatter phonons in the superconducting state. Thus, the superconducting sample's phonons are carrying heat with less resistance. This is realized as an increase in thermal conductivity just above the critical temperature. Below the critical temperature, the thermal conductivity decreases with temperature as predicted by the kinetic theory model of Equation 2. The mean free path and group velocity are basically independent of temperature because the dominant scattering processes, impurity and boundary scattering, are fixed at low temperatures. [3] C_v, and, therefore, κ, are dependent upon temperature as follows:

$$C_v \ \alpha\ T \qquad (3)$$

if electron carriers dominate and:

$$C_v \ \alpha\ T^N \qquad (4)$$

if phonon carriers dominate, where N represents the dimensionality of phonon propagation if phonon carriers dominate. Very low temperature measurements show κ depending upon T between T^2 and T^3. This suggests that the phonon contribution is dominating the thermal conductivity at low temperatures and that the dimensionality lies somewhere between 2 and 3. This reduced dimensionality is consistent with the highly anisotropic nature of the ceramic superconductors. We obtained

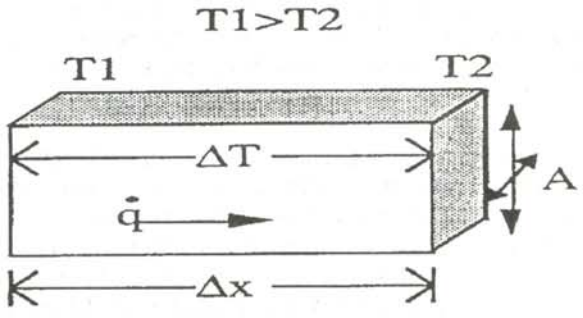

Figure 1
Quantities measured to determine the thermal conductivity.

Jim graduated with a B.Sc. in physics from Miami University. This work was completed during two summer assistantships with Professor Pechan at Miami University in Oxford, Ohio. He was recently married and is now living with his wife Lisa in Columbus, Ohio

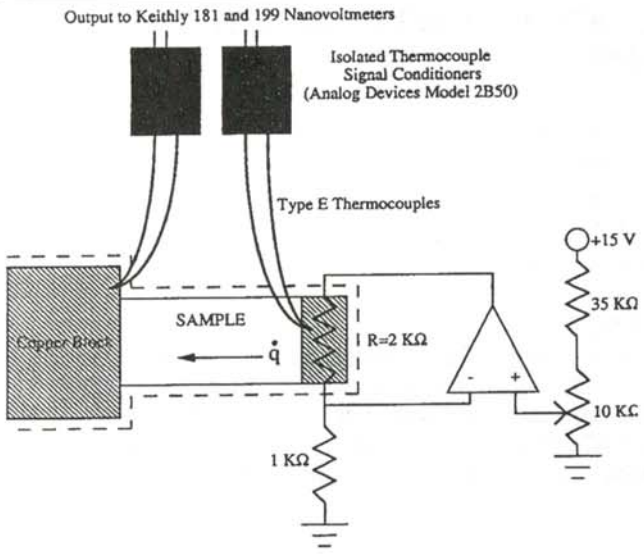

Figure 2

Experimental setup. The items inside the dashed lines were contained in the evacuated chamber of the flow through cryostat. The copper block was pressed against the bottom of the cryostat. The 2 kW resistor was imbedded in a copper block. The sample was connected to the two copper blocks with a silver based thermally conducting expoxy.

information about the chemical phase of the sample by performing resistance measurements near the transition temperature. A narrow superconducting transition width suggests the dominance of a single chemical phase, while a wide transition width implies that a mixed phase composition is present. We used the quasi-equilibrium technique [5] to obtain our measurements.

THE EXPERIMENT

The thermal conductivity for the sample was determined by measuring the various parts needed in Equation 1. Figure 1 is a drawing of our sample with approximate dimensions 3 mm x 9 mm x 16 mm. The experimental setup is shown schematically in Figure 2. Thermally conducting silver based epoxy was used to To ensure good thermal contact between the copper block and the cryostat, the probe that holds the block was spring loaded.

The thermal energy was supplied to the upper block by an embedded 2 kW resistor carrying a precisely controlled current. The current was adjusted by a potentiometer. The dial readings could be converted to a current reading using a simple linear calibration curve. The thermal power deposited by the resistor was computed using the expression:

$$dQ/dt = \text{Power} = I^2 R \qquad (5)$$

The temperature gradient $\Delta T/\Delta x$ was determined by measuring the temperature of each copper block with type

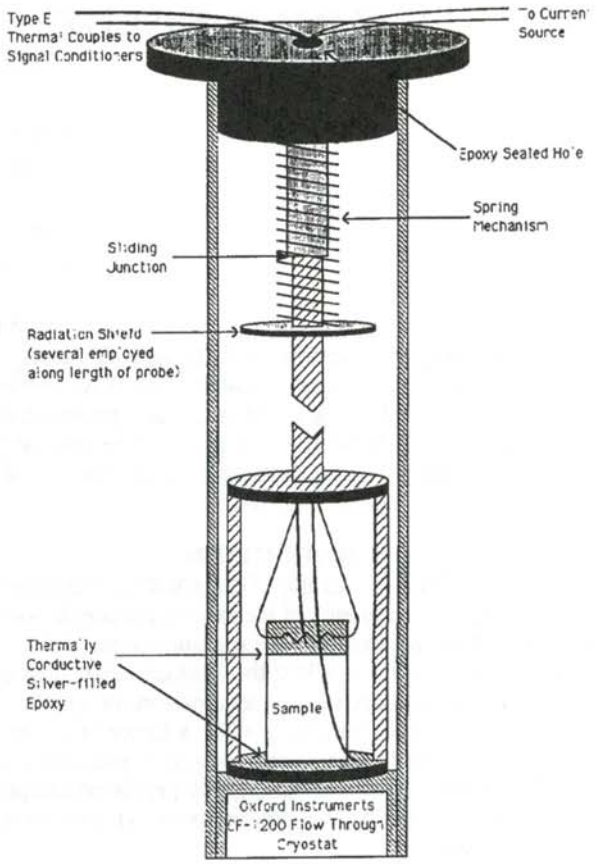

Figure 3

Experimental apparatus.

E thermocouples imbedded in them. The voltage signal from the thermocouples were amplified with signal conditioners [6] and fit to a second order polynomial in each of six 25K segments to cover the 150K range of measure-

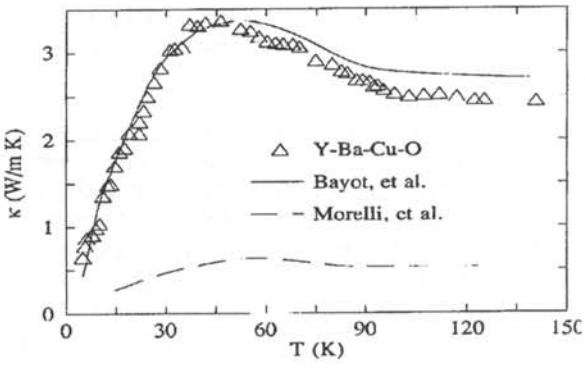

Figure 4

Thermal conductivity of $Y_1Ba_2Cu_3O_{7-x}$. The solid line is an approximate fit to the data of Bayot et.al. The dashed line is an approximate fit to the data of Morelli et.al. There is a 5% error due to the uncertainty in the thermocouple readings.

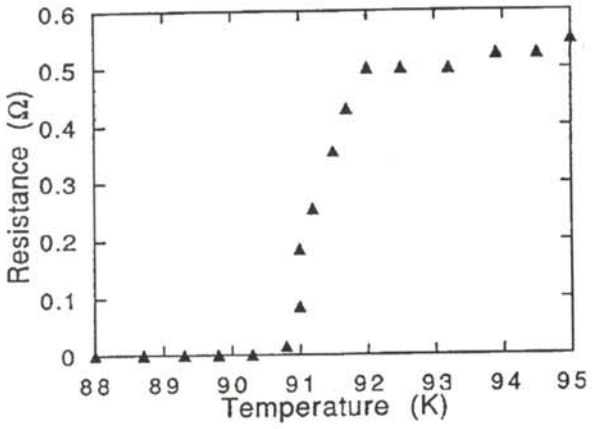

Figure 5
Resistance of our $Y_1Ba_2Cu_3O_{7-x}$ sample. Note the approximately 1K transition width.

ments. The theromcouples were calibrated at ice and liquid nitrogen temperatures. The ice-water temperature was used to determine the zero offset and the liquid nitrogen data were used to determine the gain of the thermocouple signal conditioners.

The temperature of the sample was controlled to within ±1K by a flow-through cryostat 7 with a temperature controller shown in Figure 3. The sample chamber was evacuated to 10^{-5} Torr so that the effects of conduction and convection due to the surrounding gases would be minimized. We estimated the value of κ for the chamber to be 3.1×10^{-10} W/(mK), about 9 orders of magnitude below our lowest thermal conductivity measurements. The convective heat transfer in the sample chamber was estimated at 1.3×10^{-7} W/(m²K).

Equilibrium, a stable temperature gradient, was generally obtained within 5 to 10 minutes after changing the temperature controller and adjusting the rate of heat flow. The temperature gradient was maintained at (2.0 ± .1)K, causing a 5% uncertainty in the thermal conductivity measurement.

RESULTS AND DISCUSSION

The results of our measurement of thermal conductivity of $Y_1Ba_2Cu_3O_{7-x}$ is shown in Figure 4. Our measurements are in close agreement with those made by Bayot et. al.[1]. The features of the graph are the same as those of Morelli et. al., [2] however, the magnitude of their measurement, 0.5 W/(m K) at room temperature, is significantly lower than ours. We believe that this was due to their sample being composed of mixed phases of material. They measured a transition width of approximately 5K, while our resistance measurements, shown in Figure 5, indicate a transition width of only 1K. This indicates that our measurements and the measurements of Bayot et.al, who also got 1K, are better representative of single phase $Y_1Ba_2Cu_3O_{7-x}$.

We checked our system for measuring κ by running a second sample, $Bi_2CaSr_2Cu_2O_{9-x}$, shown in Figure 6. The close agreement between our data and previous results provided a good test for our experimental technique.[8]

Some of the features of the thermal conductivity vs. temperature curve discussed in the introduction can be seen in our data. Figures 4 and 6 show the upturn in the thermal conductivity just above the transition temperature of 91K. Our measurements seem to show a linear behavior at low temperatures. However, our lowest temperature measurements are at the transition between dominance of impurity and boundary scattering and the dominance of carrier carrier- scattering.

ACKNOWLEDGMENTS

The author would like to thank Dr. Michael Pechan for his guidance and patience and Dr. Arthur Middleton for his interest and support. This work was supported by the US Department of Energy Basic Energy Sciences Contract No. DE-FG02-86EER45281.

REFERENCES

* Current address of author: 2443 Mallard's Landing Drive, Columbus, OH 43229.

1. V. Bayot, F. Delannay, C. Dewitte, J-P Erauw, X. Gonze, J-P Issi, A. Jonas, M. Kinany-Alaoui, M. Lambricht, J.P. Michenaud, J-P Minet and L. Piraux, Solid State Comm., 63, 1987, pp. 983-986.

2. D.T. Morelli, J. Heremans and D.E. Swets, Phys. Rev. B, 36, 1987, pp. 3917-3919.

3. C. Kittel, Introduction to Solid State Physics, Wiley,

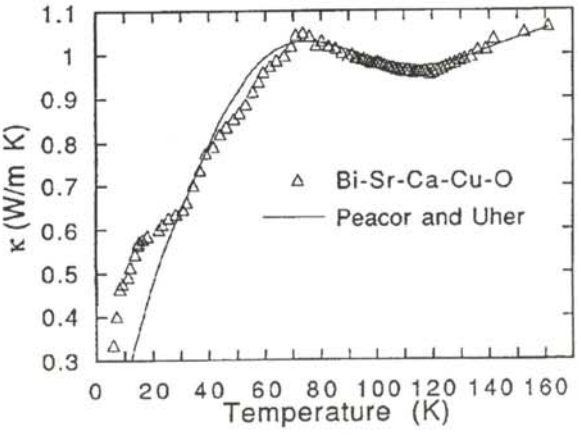

Figure 6
Thermal conductivity of $Bi_2CaSr_2Cu_2O_{9-x}$. The solid line is an approximate fit to the data of Peacor and Uher. The 5% error is due to the uncertainty in the thermocouple readings.

1986, p. 121.

4. J.J. Freeman, T.A. Friedmann, d.M. Ginsberg, J. Chen, and A. Zangvil, Phys. Rev. B, 36, 1987, pp. 8786-8787.

5. M.J. Pechan and J.A. Horvath, Am. Jour. Phys., 58, 1990, pp 642-644.

6. Analog Devices Model 2B50A and 2B50B thermocouple signal conditioners.

7. Oxford Instruments CF 1200 flow-through cryostat with a ITC-4 temperature controller.

8. S.D. Peacor and C. Uher, Phys. Rev. B, 39, 1989, pp 11,559-11,562.

FACULTY SPONSOR

Dr. Michael J. Pechan
Department of Physics
Miami University
Oxford, OH 45056

PRECESSION IN NEWTONIAN GRAVITATION, GENERAL RELATIVITY AND PSEUDO-NEWTONIAN GRAVITATION

Brent Scales * and Kevin Cornelius
Department of Physics
Southern Nazarene University
Bethany OK 73008

received December 19, 1992

ABSTRACT

The precession of the elliptical trajectory for a particle bound to a center of force by the potential A/r + B/r^2 + C/r^3 is calculated. Three theories are compared for their precessional predictions: Newtonian gravity; corrections to Newtonian theory coming from general relativity; and a non-linear 'pseudo-Newtonian' model which is a hybrid of Newtonian theory and special relativity. The latter has qualitative features in common with general relativity, such as the contribution of the electric field to gravitation when the central body carries an electric charge and precession about the central body even if it is a point source. However, this precession is quantitatively incorrect. Since the Newtonian and pseudo-Newtonian models deploy only the vector field $\vec{g}$ and the scalar field Φ (the potential), our results confirm that at least a second-rank tensor field may be required for a successful relativistic theory of gravitation.

A Generic Study of Precession

The precession in the elliptical orbit of a satellite of mass m can be calculated in the following manner. The trajectory is given in polar coordinates by:

$$\theta = \sqrt{\frac{L^2}{2m}} \int \frac{dr}{r^2 \sqrt{E - V(r) - \frac{L^2}{2m}}} \qquad (1)$$

where E is the satellite's mechanical energy, L its angular momentum, V(r) = m Φ(r) is its potential energy, m is the reduced mass of the system and r is the relative coordinate. If the satellite is trapped in the gravitation potential:

$$\Phi(r) = \frac{A}{r} + \frac{B}{r^2} + \frac{C}{r^3} \qquad (2)$$

Equation 1 can be written as:

$$\theta = -\sqrt{\beta'} \int \frac{du}{\sqrt{E + \alpha u - \beta u^2 + \gamma u^3}} \qquad (3)$$

where

$$u = \frac{1}{r} \qquad \alpha = -mA \qquad \beta = mB + \frac{L^2}{2m}$$
$$\beta' = \frac{L^2}{2m} \qquad \gamma = -mC \qquad (4)$$

Notice that $\beta = \beta'$ if and only if $B = 0$. If C, and thus γ, is small, expanding the integrand of Equation 3 in powers of γ and then evaluating the integral gives: [3]

$$\theta \approx \sqrt{\frac{\beta'}{\beta}} \left[1 + \frac{3\alpha\gamma}{4\beta^2}\right] \sin^{-1}\left\{\left(1 - \frac{2\beta}{r\alpha}\right)\frac{1}{e}\right\} + F(r) + constant, \qquad (5)$$

where

$$e = \sqrt{1 + \frac{4\beta E}{\alpha^2}} \qquad (6)$$

is the eccentricity and $F(r)$ is a complicated non-periodic function of r. [2] $F(r)$ can be approximated by $F(a)$, where a is the length of the semi-major axis. It then can be absorbed into the integration constant which can be made to vanish by an appropriate choice of initial conditions. [3] Equation 5 then becomes:

$$\frac{1}{r} = \frac{\alpha}{2\beta}\left\{1 - e \sin\left[\frac{\theta\sqrt{\frac{\beta}{\beta'}}}{1 + \frac{3\alpha\gamma}{4\beta^2}}\right]\right\}. \qquad (7)$$

The radial coordinate r regains its original value when the argument of the sine function increases by 2π, so that the change in the polar angle, $\Delta\theta$, for a complete cycle of the orbit is given by:

Brent graduated from Southern Nazarene University in January 1993 with a B.Sc. in physics. This research was done during his senior year and was presented at several regional Society of Physics Students meetings. Brent now works as a programmer in Research and Development at DataRay Inc. in Oklahoma City.

Kevin is a senior physics and math major at Southern Nazarene University. He plans to earn a Ph.D. in acoustical physics.

$$\frac{\Delta\theta\sqrt{\frac{\beta}{\beta'}}}{1+\frac{3\,\alpha\,\gamma}{4\,\beta^2}}=2\,\pi\,, \tag{8}$$

or

$$\Delta\theta=2\,\pi\sqrt{\frac{\beta'}{\beta}}\left[1+\frac{3\,\alpha\,\gamma}{4\,\beta^2}\right]. \tag{9}$$

The precession angle, δ, then can be found:

$$\delta=\Delta\theta-2\,\pi$$
$$=2\,\pi\left\{\left(\sqrt{\frac{\beta'}{\beta}}-1\right)+\sqrt{\frac{\beta'}{\beta}}\,\frac{3\,\alpha\,\gamma}{4\,\beta^2}\right\} \tag{10}$$

So, if one knows the constants A, B and C in Equation 2, one can calculate the precession angle for the orbit. We will examine three different models for gravitation: Newtonian; general relativity; and a 'pseudo-Newtonian' gravity that is a non-linear hybrid of special relativity and Newtonian theory. For each theory, the gravitational potential is calculated to order $1/r^3$, thereby determining the coefficients in Equation 1 and then computing the precession using Equation 10.

Newtonian Gravitation

The Newtonian gravitational potential is:

$$\Phi(r)=-G\int\frac{\rho(\vec{r}')}{\left|\vec{r}-\vec{r}'\right|}\,d^3r' \tag{11}$$

where $\boldsymbol{r}$ - $\boldsymbol{r}'$ is the vector from the source point $\boldsymbol{r}'$ to the field point $\boldsymbol{r}$, $\rho(\boldsymbol{r}')$ is the mass density and G is Newton's gravitational constant. Performing a binomial expansion of $\frac{1}{\left|\vec{r}-\vec{r}'\right|}$ about $\mathrm{F}'=0$, we obtain the multipole expansion [4]:

$$\Phi(r)=-\frac{GM}{r}-G\frac{\left(\hat{r}\cdot\vec{D}\right)}{r^2}-\frac{1}{2}\,G\sum_{n,k}\frac{Q_{nk}\hat{r}_n\cdot\hat{r}_k}{r^3}+\ldots \tag{12}$$

where

$$M=\int\rho(\vec{r}')\,d^3r' \tag{13}$$

is the total mass of the source,

$$\vec{D}=\int\vec{r}'\;\rho(\vec{r}')\,d^3r' \tag{14}$$

is its gravitational dipole moment and

$$Q_{nk}=\int\left(3\,r'_n\,r'_k-r'^2\,\delta_{nk}\right)\rho(\vec{r}')\,d^3r' \tag{15}$$

are the components of its quadrupole tensor. If the center of mass is at the origin, D vanishes. Newtonian gravitational sources do not have gravitational dipole moments. This means that the constant B in Equation 2 vanishes. Thus, a Newtonian source will produce precession in a satellite's orbit only if the source has a quadrupole moment, thus breaking the spherical symmetry.

General Relativity

In general relativity, the first non-zero correction to the Newtonian gravitational potential energy of a point mass m in the field of a point source of mass M includes a $1/r^3$ term. To this order [5], the potential energy can be written as:

$$V(r)=-\frac{G\,M\,m}{r}-\frac{G\,M}{c^2}\,\frac{L^2}{m}\,\frac{1}{r^3}+\ldots \tag{16}$$

where c is the speed of light. Here again, $B=0$. From Equation 10, one obtains the famous result for the precession angle

$$\delta_{rel}=\frac{6\,\pi\,G\,M}{a\,c^2\,(1-e^2)} \tag{17}$$

Putting in the appropriate numbers for the planet Mercury, Equation 17 gives about 43 seconds of arc per century, which is in agreement with observations.

Pseudo-Newtonian Gravitation

This model is a non-linear hybrid of special relativity and Newtonian theory. Just as the 'old quantum theory' that was based on the Bohr-Sommerfield-Wilson quantizaton rules was a hybrid classical/quantum theory of the atom, this 'pseudo-Newtonian gravitation' is a conceptual patchwork that is intermediate between classical gravitation and general relativity. As with the old quantum theory, pseudo-Newtonian gravitation is not always successful quantitatively, but contains some conceptual features that survive in the more comprehensive theory.

Pseudo-Newtonian gravitation begins with Poisson's equation for the Newtonian potential:

$$\nabla^2\,\Phi=4\,\pi\,G\,\rho_{mass} \tag{18}$$

where ρ_{mass} is the mass density of the source. Now we fold in the idea from special relativity that a mass m is an energy mc^2. Hence, the gravitational field energy density

$$-\frac{\vec{g}^2}{8\,\pi\,G} \tag{19}$$

corresponds to a 'mass density equivalent' of the gravitational field:

$$\rho_{gravity\ field}=-\frac{\left(\nabla\Phi\right)^2}{8\,\pi\,G\,c^2} \tag{20}$$

Pseudo-Newtonian gravitation is invented [6] by including $\rho_{\text{gravity field}}$ in the source term of Equation 18

$$\nabla^2\,\Phi=4\,\pi\,G\left(\rho_{mass}+\rho_{field}\right) \tag{21}$$

This model has been extended [7] to include a source carrying an electric charge q, so that ρ_{field} would include the mass equivalent of the electric field energy density

$$\rho_{electric\ field}=\frac{1}{2}\,\frac{E^2}{c^2}=\frac{1}{2}\,\frac{\left(\nabla\varphi\right)^2}{c^2} \tag{22}$$

(in Lorentz-Heaviside units), where φ is the electric potential.

Consider a satellite of mass m and zero electric charge, moving in the $\boldsymbol{g}$ and $\boldsymbol{E}$ fields of a point mass M that carries a charge q. In the neighborhood of the satellite, where there is no source mass, so that $\rho_{mass} = 0$, Equations 20 - 22 reduce to the non-linear equation:

$$\nabla^2\Phi + \frac{1}{2c^2}(\nabla\Phi)^2 = \frac{1}{2}\sigma^2 c^2 (\nabla\varphi)^2, \qquad (23)$$

where

$$\sigma = 2\frac{\sqrt{\pi G}}{c^2} \qquad (24)$$

When the Coulomb potential is used for φ, the solution to this equation has been found to be [7]

$$\Phi(r) = 2c^2 \ln\left\{\exp\left(\frac{\sigma q}{2r}\right) - \left[1 + \frac{GM}{\sigma q c^2}\right]\sinh\left(\frac{\sigma q}{2r}\right)\right\}, \qquad (25)$$

We now will expand this solution to order $(1/r^3)$ so that we can use the parameterization of Equation 2 to find the precession of the satellite in this pseudo-Newtonian gravitational potential. We find:

$$A = -GM \qquad (26)$$

which reduces to the Newtonian limit, and

$$B = \pi G\frac{q^2}{c^2} - \left(\frac{GM}{2c}\right)^2$$

$$C = -\pi\frac{M}{3}\left(\frac{Gq}{c}\right)^2 + \frac{(GM)^3}{12c^4} \qquad (27)$$

Since $B \neq 0$, even if $q = 0$, it appears that the pseudo-Newtonian gravitation model predicts a gravitational dipole moment for a point source. This is in contrast to the Newtonian theory and the limit of the general relativistic model.

We now can use Equation 11 to find the precession angle, δ_{pn}, predicted by pseudo-Newtonian gravitation. δ_{pn} is related to the general relativistic precession angle δ_{rel}, given in Equation 17 by:

$$\delta_{pn} = \frac{\delta_{rel}}{12} - \frac{(\delta_{rel})^2}{72\pi} \approx \frac{\delta_{rel}}{12} \qquad (28)$$

This would predict a precession angle for Mercury that is a factor of 12 smaller than the measured one.

DISCUSSION

The pseudo-Newtonian model is 'on the right track' is some qualitative ways, but is quantitatively incorrect. As with general relativity, where all energy sources produce gravitational fields, the pseudo-Newtonian model has an contribution to the gravitational potential from the electric interaction. As with general relativity, the pseudo-Newtonian model predicts precession for the orbit of a satellite around a point source. However, the magnitude of the precession predicted by the pseudo-Newtonian model is significantly less that measured.

A relativistic theory of gravitation requires more than 'Newtonian gravitation plus $E = mc^2$'. One should not be surprised than general relativity is more complicated than Newtonian gravitation and special relativity. The pseudo-Newtonian model is useful, as shown in our calculation that it produces a precession of the orbit, for showing why this is so.

The underlying problem with the pseudo-Newtonian model is that, as with the Newtonian theory, it attempts to model gravitational fields with only a zero and a first rank tensor (the gravitational potential Φ and the vector field g respectively). This example suggests than an accurate relativistic model of gravitational, viz. general relativity, must contain at least a second-rank tensor.

REFERENCES

* present address of author: 318 Douglas Drive, Midwest City, OK, 73110

1. J. Marion, Classical Dynamics of Particles and Systems, Academic Press, New York, 1970, Chapter 8.

2. G. Bois, Tables of Indefinite Integrals, Dover, New York, 1961, p. 70.

3. K. Doggett, American Journal of Physics, 59, 1991, pp. 851-852.

4. H. Ohanian, Gravitation and Spacetime, Norton, New York, 1976, pp. 10 - 11.

5. J. Marion, Classical Dynamics of Particles and Systems, Academic Press, New York, 1970, Chapter 4.

6. P. Peters, American Journal of Physics, 49, 1981, pp. 564 - 569.

7. J. Young, American Journal of Physics, 59, 1991, pp. 565-567.

FACULTY SPONSOR

Dr. Dwight E. Neuenschwander
Department of Physics
Southern Nazarene University
Bethany, OK 73008

NEUTRON SCATTERING: Constant Magnetic Field Band

Thomas D. Burnes II and Scott L. Stenberg
Physics Department
University of Nebraska at Omaha
Omaha, NE 68182-0266
received December 19, 1992

ABSTRACT

The exact solutions to the Pauli spinor equations which give rise to the transmission and reflection coefficients for a neutral magnetic dipole in a constant magnetic field band are presented. Since the parallel and antiparallel spin components see different potential barriers that depend totally on their orientations with the external magnetic field, it is possible to use this spin-dependent feature to study the characteristics of the magnetic field. Two examples of the transmission and reflection coefficients for both spin states are presented.

INTRODUCTION

Stern and Gerlach[1] first observed a splitting of a neutral silver atomic beam after it was passed through an inhomogeneous magnetic field. This result indicated the existence of only two possible orientations for the magnetic moment of the silver atoms. In 1925, Uhlenbeck and Goudsmit[2] attributed the shift of the magnetic moment of the electron to its intrinsic angular momentum. This hypothesis of the electron spin proved to be correct and is now regarded as one of the fundamental properties of all elementary particles.

By analogy, it is required that the spin angular momentum operators of S_x, S_y, and S_z must also satisfy the same quantum mechanical commutation relation of that of the orbital angular operators, that is, for L_x, L_y, and L_z, which are functions of the angle variables θ and ϕ,

$$L_xL_y - L_yL_x = i\hbar L_z . \tag{1}$$

We must have the similar commutation relation for spin angular momentum operators:

$$S_xS_y - S_yS_x = i\hbar S_z . \tag{2}$$

Pauli introduced the matrix representation for these operators which satisfy Equation 2:

$$S_x = \frac{1}{2}\begin{pmatrix} 0 & 1 \\ 1 & 0 \end{pmatrix}, S_y = \frac{1}{2}\begin{pmatrix} 0 & i \\ i & 0 \end{pmatrix}, S_x = \frac{1}{2}\begin{pmatrix} 1 & 0 \\ 0 & -1 \end{pmatrix}. \tag{3}$$

$$S_xS_y - S_yS_x = i\hbar S_z .$$

The eigenfunctions of the orbital angular momentum operators L_x, L_y and L_z are continuous functions of the angle variables θ and ϕ while the spin angular momentum operators S_x, S_y, and S_z, given in Equation 3, are 2 x 2 matrices. The eigenvectors of S_x, S_y and S_z are column vectors. For example the spin states for the positive z and the negative z directions are:

$$\chi_z = \begin{pmatrix} 1 \\ 0 \end{pmatrix} \quad , \quad \chi_{-z} = \begin{pmatrix} 0 \\ 1 \end{pmatrix}. \tag{4a}$$

The eigenstates for other spin-angular momentum operator, such as S_x which corresponds to spin pointing at $+x$ or $-x$ directions are:

$$\chi_{+x} = \frac{1}{\sqrt{2}}\begin{pmatrix} 1 \\ 1 \end{pmatrix}, \quad \chi_{-x} = \frac{1}{\sqrt{2}}\begin{pmatrix} 1 \\ -1 \end{pmatrix} \tag{4b}$$

and for the spins pointing in the y direction:

$$\chi_{+y} = \frac{1}{\sqrt{2}}\begin{pmatrix} 1 \\ i \end{pmatrix}, \quad \chi_{-y} = \frac{1}{\sqrt{2}}\begin{pmatrix} 1 \\ -i \end{pmatrix}. \tag{4c}$$

One can see that χ_{+x} and χ_{-x} are linear combinations of χ_{+z} and χ_{-z}. One can also verify that the eigenstates of S_y have the similar feature. This is entirely a quantum mechanical phenomenon.

Figure 1 shows a hypothetical experiment we proposed as a demonstration of such a novel feature. We began by utilizing a polarized neutron beam emerging from the left carrying momentum in the $+x$ direction. The neutron spin is either pointing in the $+y$ or $-y$ direction (that is, either pointing into or out of the page). The neutron then enters constant magnetic field, $\boldsymbol{B}$, which is confined to the region

Tom received his B.Sc. degree in physics in January 1993 from the University of Nebraska at Omaha. Currently, he works as a research assistant in the Department of Geophysics at UCLA.

Scott is a senior in engineering physics. He will graduate at the end of this academic year. He plans to continue his study in engineering in the graduate school. The research discussed in this paper was the product of their senior projects.

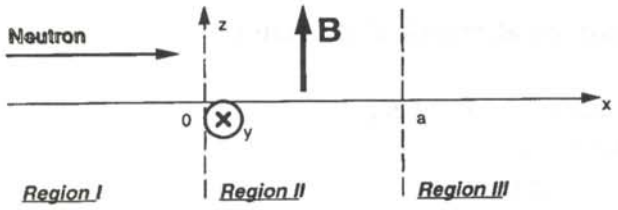

Figure 1
Schematic diagram of the hypothetical neutron scattering experiment.

from x = 0 to x = a, and points in the +z direction. The neutron beam then enters the region $x \geq a$, where there is no magnetic field. We calculate the reflection and transmission coefficients for this beam of neutrons.

THEORY AND DISCUSSION

The neutron is of monochromatic energy given by:

$$E = \frac{\hbar^2 k^2}{2m} , \qquad (5)$$

where m is the mass of the neutron, h is Planck's constant and k is the wave vector. The energy of the interaction between the magnetic moment of neutron μ_n with the magnetic field **B** is determined by:

$$U = -\vec{\mu_n} \bullet \vec{B} \quad ,where \ \mu_n = -1.91\left(\frac{e\hbar}{2mc}\right) . \qquad (6)$$

The negative sign in μ_n is due to the special property of a neutron; the direction of the magnetic moment of the neutron was found experimentally to be opposite to that of its spin angular momentum.

In contrast to classical mechanics, neutrons whose spins are pointing in the +y or -y directions in region I, have their spin components parallel or anti-parallel to the magnetic field (the z direction) in region II. If the magnetic moment is pointing opposite to the magnetic field, the total energy of the system becomes:

$$E_{\uparrow} = \frac{\hbar^2 k^2}{2m} - \mu_n B . \qquad (7)$$

In this case, the energy of a neutron decreases when it passes through the magnetic field region. It is as if a free particle sees a potential barrier of height $\mu_n B$.

The other spin component, which is opposite to the z-direction magnetic field or has the magnetic moment pointing along the magnetic field, has its energy given by:

$$E_{\downarrow} = \frac{\hbar^2 k^2}{2m} + \mu_n B . \qquad (8)$$

In this case, the energy of the neutron increases and can be viewed as a free particle passing through a well of depth $\mu_n B$.

We can use the standard mathematical treatment of a free particle passing through a potential barrier or well to describe this scattering experiment. The effect of the spin of the neutron is incorporated into the Schrödinger equation by multiplying the plane wave part by the spin state:

$$\psi = e^{ikx}\chi . \qquad (9)$$

Neutrons are sent from the left hand side, region I, where x<0, giving rise to the wave functions:

$$\psi_{+z} \ \alpha \ e^{ikx}\begin{pmatrix}1\\0\end{pmatrix} \quad and \quad \psi_{-z} \ \alpha \ e^{ikx}\begin{pmatrix}0\\1\end{pmatrix} \qquad (10)$$

for the spins parallel and anti-parallel to the magnetic field.

At the boundary between regions I and II, when x=0, there is a reflection term in the wave equations. The reflected wave is traveling in the - x direction, so the unnormalized wavefunction for spin parallel to the magnetic field can be written as:

$$\psi_{+z} = e^{ikx}\begin{pmatrix}1\\0\end{pmatrix} + R_+ e^{-ikx}\begin{pmatrix}1\\0\end{pmatrix} \qquad (11)$$

and for spin anti-parallel to the magnetic field:

$$\psi_{-z} = e^{ikx}\begin{pmatrix}0\\1\end{pmatrix} + R_- e^{-ikx}\begin{pmatrix}0\\1\end{pmatrix} , \qquad (12)$$

where R_+ and R_- are the reflection coefficients of the spin parallel and anti-parallel states respectively.

For the neutrons which penetrated the first boundary and pass through the magnetic field region, the static magnetic field does not alter the direction of the spin. The wave function in region II for the spin parallel to the magnetic field is:

$$\psi_{+z} = A_+ e^{ik'_+x}\begin{pmatrix}1\\0\end{pmatrix} + B_+ e^{-ik'_+x}\begin{pmatrix}1\\0\end{pmatrix} \qquad (13)$$

and for spin anti-parallel to the magnetic field is:

$$\psi_{-z} = A_- e^{ik'_-x}\begin{pmatrix}0\\1\end{pmatrix} + B_- e^{-ik'_-x}\begin{pmatrix}0\\1\end{pmatrix} , \qquad (14)$$

where:

$$\frac{\hbar^2 k'^2_{\pm}}{2m} = \frac{\hbar^2 k^2}{2m} \mp \mu_n B . \qquad (15)$$

In the region III, where x>a, there was no reflection, therefore, the wave is only moving in the +x direction. The wave functions in region III are:

$$\psi_{+z} = T_+ e^{ikx}\begin{pmatrix}1\\0\end{pmatrix} \quad and \quad \psi_{-z} = T_- e^{ikx}\begin{pmatrix}0\\1\end{pmatrix} \qquad (16)$$

for spin parallel and anti-parallel to the magnetic field, where $T_{\pm}$ are the transmission coefficients for the spin up and down cases respectively.

The coefficients $A_{\pm}$ and $B_{\pm}$ in Equations 13 and 14 can be determined by applying the boundary conditions at x = 0

and $x = a$ to Equations (11) through (16). The quantities of interest are the reflection and transmission coefficients R and T. They can be determined by matching the boundary conditions for both wave functions and momenta at $x = 0$ and $x = a$. This is identical to the quantum mechanical treatment of a free particle passing through a potential barrier or well. However, in this case, the equations must be matched separately for the spin parallel and spin anti-parallel cases.

Since the kinetic energy of the incident neutron can be either greater than or less than the potential barrier, there were two different situations to address. In the case when the spin is parallel to the magnetic field, the barrier could be larger or smaller than the kinetic energy of the neutron. When the spin is anti-parallel to the magnetic field, the barrier is always less than the kinetic energy.

For the case when the spin is parallel to the field and when the barrier term is greater than E, the equation for reflectivity is:

$$R = |R_+|^2 = \left[1 + 4\zeta(1+\zeta)(\sinh k'a)^{-2}\right]^{-1} \qquad (17)$$

and the equation for transmissivity is:

$$R = |R_+|^2 = \left[1 + 4\zeta(1+\zeta)(\sinh k'a)^{-2}\right]^{-1} \qquad (17)$$

where:

$$\zeta = \frac{E}{\mu_n B} \qquad (19)$$

and:

$$k' = \sqrt{\frac{2m\mu_n B}{\hbar^2} - k^2}\,. \qquad (20)$$

After some algebraic manipulation, one finds that:

$$R + T = 1 \qquad (21)$$

which guarantees the conservation of particle flux.

Now consider the case where kinetic energy is greater than the barrier. The equation for reflectivity is:

$$R = |R_+|^2 = \left[1 + 4\zeta(\zeta-1)(\sin k'a)^{-2}\right]^{-1} \qquad (22)$$

and the equation for transmissivity is:

$$T = |S_+|^2 = \left[1 + \frac{\sin^2 k'a}{4\zeta(\zeta-1)}\right]^{-1}\,. \qquad (23)$$

In this case, the value for k′ is given by:

$$k' = \sqrt{k^2 - \frac{2m\mu_n B}{\hbar^2}}\,. \qquad (24)$$

One can see that when the barrier is larger than the kinetic energy, R and T (Equations 17 and 18) vary exponentially with energy. But when barrier term is less than the kinetic energy, R and T (Equations 22 and 23) oscillate with E.

In the spin down case there is only one possibility because the incident energy is always above the potential well. In this situation k' becomes:

$$k' = \sqrt{k^2 + \frac{2m\mu_n B}{\hbar^2}}\,. \qquad (25)$$

The equation for reflectivity is:

$$R = |R_-|^2 = \left[1 + 4\zeta(1+\zeta)(\sin k'a)^{-2}\right]^{-1} \qquad (26)$$

and the transmissivity is:

$$T = |S_-|^2 = \left[1 + \frac{\sin^2 k'a}{4\zeta(1+\zeta)}\right]^{-1}\,. \qquad (27)$$

Once again, we find that:

$$R + T = 1\,. \qquad (28)$$

Finally, when

$$k'a = n\pi \quad , \quad n = 1, 2, 3, \ldots \qquad (29)$$

$R = 0$ and $T = 1$. This is the resonant transmission, the case where the reflected wave disappears.

NUMERICAL RESULTS

Computer programs were written to generate data and graphs for the various reflectivity and transmissivity coefficients as a function of energy. Figure 2 shows the transmissivity and reflectivity for $B = 50$ T, the highest magnetic field produced in laboratories, in the energy range of 4.0 x 10^{-25} J to 8.0 x 10^{-25} J and magnetic field band spacing $a = 2.7$ x 10^{-8} m. Figure 3, shows the transmissivity and reflectivity coefficients for $B = 8.0\text{x}10^{+8}$ Gauss, the magnetic field of a typical neutron star,

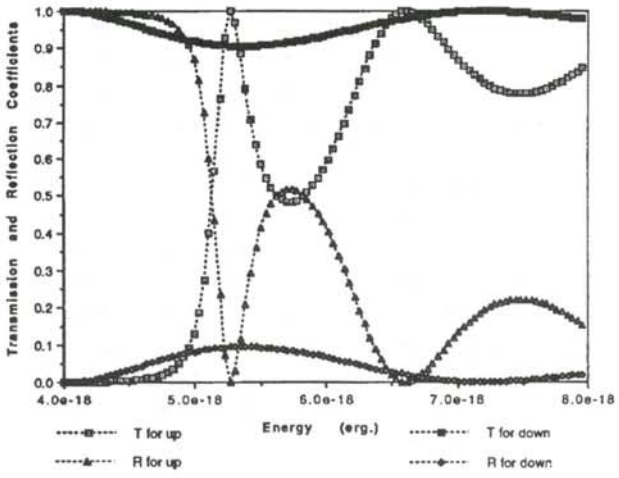

Figure 2

Reflectivity and transmissivity coefficients for a magnetic field of 50 T confined to a spacing of 2.7 x 10^{-8} m. Notice the oscillatory behavior.

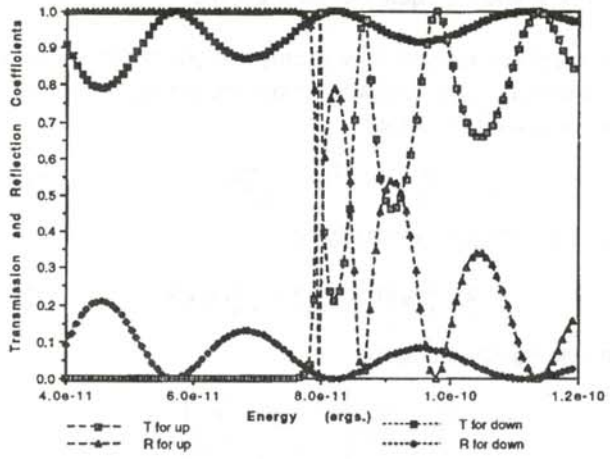

Figure 3

Transmissivity and reflectivity coefficients for a magnetic field of 8.0 x 10^8 T and a magnetic field band spacing of 1.2 x 10^{-11} m, values typically found in a neutron star.

in an energy range of 4.0 x 10^{-18} J to 1.2 x 10^{-17} J and a magnetic field band spacing a = 1.2 x 10^{-11} m. The values of the magnetic field band width and energy ranges were chosen to demonstrate oscillatory behaviors. The kinetic energies were chosen to be on the order of magnetic interaction energies $\mu_n B$ and magnetic field band widths were of the order of the reciprocal of the wave vectors. The amplitudes of oscillation for the spin parallel to the magnetic field cases were smaller than those of the anti-parallel cases. This is because the neutrons have different energy while passing through the magnetic field.

SUMMARY

The mathematical formulation of quantum wave scattering by the square potential barrier and well was used to describe the interaction of a neutron spin in a constant magnetic field. Exact equations for reflectivity and transmissivity were derived which indicated that when the spin is parallel to the magnetic field, the neutron sees a barrier and when the spin is anti-parallel to the magnetic field, the neutron sees a well. A computer program was developed to generate data for analysis. Plotting of the data revealed the expected results. Recently Barut and Dowling [3] studied the energy band structure using the neutral magnetic dipole scattering through a periodic magnetic field. They suggest to utilize this spin dependent effect as a spin-polarizer. The purpose of our independent study was to use neutrons as a probe to study the magnetic field distribution inside the flux tube and the structure of the flux tube of the type-II superconductors.

REFERENCES

1. O. Stern and W. Gerlach, Z. Phys., 8, 1921, p. 110; Z. Phys.,9, 1922, pp. 349-352.

2. G.E. Uhlenbeck and S. Goudsmit, Naturwiss, 13, 1925, p. 953 ; Nature 117, 1926, p. 264.

3. A.O. Barut and J.P. Dowling, Phys. Rev. Lett. 68, 1992, p. 3571.

FACULTY SPONSOR

Dr. Wai-Ning Mei
Department of Physics
University of Nebraska at Omaha
Omaha, NE 68182-0266

CROSS SECTION MEASUREMENTS OF THE $^{90}Zr(n,p)^{90m}Y$ REACTION FROM 5.4 MeV to 12.3 MeV

Szabolcs Márka*
Institute of Experimental Physics
Kossuth Lajos University
P.O.B. 105
Debrecen 4001, Hungary
received January 11, 1993

ABSTRACT

This work is part of an experimental program that measured the excitation functions for several reactions of Zr isotopes. This paper is a study of the $^{90}Zr(n,p)^{90m}Y$ process using the foil activation technique. Neutrons were produced by the $^{2}H(d,n)^{3}He$ reaction using a D_2 gas target. The deuterons were accelerated with a variable energy cyclotron. Foils were irradiated by mono-energetic neutrons. The activity of the foils was determined using a semiconductor g-detector. The neutron flux density was quantified using $^{27}Al(n,\alpha)$ and $^{56}Fe(n,p)$ reactions. We measured the cross section at several energies and obtained results in a previously unexplored energy range. Our results were consistent with older results at lower energies.

INTRODUCTION

Experiments that determine the excitation function for several neutron induced nuclear reactions have been performed for many decades at the Institute of Experimental Physics at the Kossuth Lajos University (KLTE) [1].

From my childhood I was interested in the natural sciences. In the secondary school, I studied computers and programming intensively. After competing in the entrance examination to the KDK (Research Student Circle) I had a chance to participate in research at the university as a high school junior.

After completing my compulsory military service, I was accepted to Kossuth Lajos University in mathematics and physics. In the second semester at the university, I joined a research group in the Experimental Physics Department. The first results of this experiment was presented at the 1991 National Science Student Conference.

During the last year, one of my friends and I also studied red sensitive holographic emulsions and reflection holograms. Beginning in the autumn of 1991, I was a teaching assistant and taught introductory physics labs for freshmen. For two months during the fall of 1992, I was a visiting student at the University of Alabama, Tuscaloosa. From November 1992 to February 1993 I spent three months at the University College of Sawasea, Wales. I graduated in June, 1993 from Kossuth Lajos University, Debrechen. Currently, I am a graduate student in the United States

This paper is a discussion of an experiment in which the excitation function for the $^{90}Zr(n,p)^{90m}Y$ reaction was determined. Zr is an interesting target because this metal is abundant in a number of situations where there is a very high neutron flux, e.g. in fission reactors. Also, the excitation function for Zr has been examined in only a few experiments.

We determined the cross section of the reaction in the following way. We irradiated the Zr foil and the monitor foils with mono-energetic neutrons for a fixed length of time. The Y produced in the (n,p) reaction is in an excited state. It decays to the ground state by gamma emission with a characteristic spectrum. By measuring the number of gammas produced in the decay, the absolute number of Y nuclei produced from the neutron irradiation can be determined. From this value, the neutron flux (determined using monitor foils with well-known excitation functions), the time of irradiation, and from some geometric factors, we could find the cross section for the $^{90}Zr(n,p)^{90m}Y$ reaction.

THE EXPERIMENT

If one needs mono-energetic neutrons in the few MeV range at several energy points, an accelerator is used. The neutrons are produced by accelerating mono-energetic deuterons at a deuterium target and making use of the $^{2}H(d,n)^{3}He$ reaction. The neutrons produced are mono-energetic because the incident deuterium beam is mono-energetic and ^{3}He has no discrete excited states. The deuterons were produced by the MGC20 cyclotron [2] with a beam current of 3 μA. This machine is isochronous, compact and can be used for producing deuterons with about 10 MeV energy with a small energy spread. We used

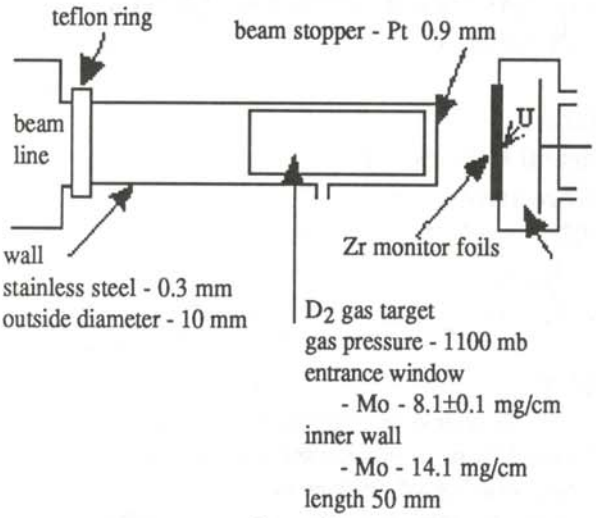

Figure 1

Position of the gas target, the fission chamber and the foils. The characteristics of the D_2 garget are shown.

neutron energy (MeV)	flux 10^6 cm^{-2}s^{-1}	s mm	irradiation time in hrs	BG
5.38±0.18	16.47	15	6.84	No
5.89±0.18	16.02	15	6.85	No
6.39±0.18	12.82	15	8.93	No
6.80±0.18	14.46	15	4.33	No
8.02±0.09	5.49	40	7.19	No
8.43±0.09	5.83	40	6.89	No
8.92±0.17	15.04	20	3.65	No
9.43±0.09	2.05	40	10.10	No
10.23±0.09	4.82	40	6.23	Yes
10.95±0.09	5.57	40	7.33	Yes
11.56±0.09	3.89	40	5.19	Yes
12.25±0.10	7.04	40	6.18	Yes

Table 2

Characteristics of the various irradiations. s is the distance between the foil and the end of the gas target. The column BG indicates if there was background irradiation with an empty gas target.

a D_2 gas target. The gas pressure fluctuated about 100 mbar because in this case, the D_2 gas in the target cannot get polluted by the gas outside the target. The experimental setup is shown in Figure 1.

The $^2H(d,n\,p)^2H$ reaction causes background problems above 5 MeV. We also had to take into account that the Mo entrance window of the gas chamber changed the energy and energy spread of the deuterons. The energy and energy spread of the neutrons for the given geometry was calculated by the Monte Carlo method.

The neutron flux density was measured by the foil activation technique. The essence of the method is that the foils of different metals are irradiated together with the Zr foil by identical neutron fluxes. If we know the exact excitation function of these monitors, we can calculate the absolute neutron flux density. From that, we can determine the unknown excitation function. The monitor foils used are listed in Table 1.

We followed the variations of the neutron flux density with a fission chamber during the irradiation process. The position of this instrument is shown in Figure 1. We

Metal	Mass (grams)	Thickness (mm)
In	0.54	0.27
Al	0.14	0.2
Fe	0.22	0.1
Zr	1.75	1.1
Ni	2.5	1.0

Table 1

List of fils used. Each foil had a diameter of 19mm.

mounted the foils on the front part of the chamber, tight to the ^{238}U layer. The ^{238}U coating of the chamber contains 0.03% ^{235}U. Its mass is 538 μg and has a diameter of 19 mm. The temperature of the target was monitored with a thermocouple. The target was isolated from the beam transport system by a teflon ring so that the target current

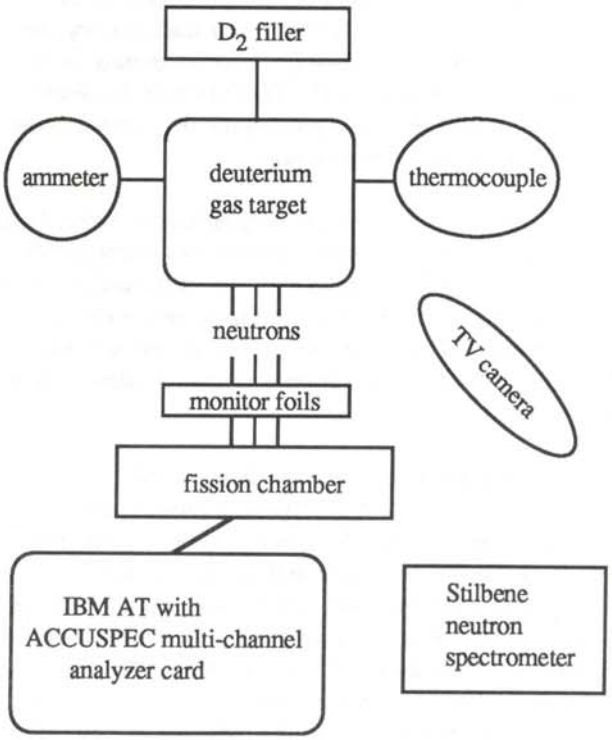

Figure 2

Schematic diagram of the devices used during irradiation.

Reaction	A %	Half-life hours	E_γ keV	I_γ %
$^{90}Zr(n,p)^{90m}Y$	51.12	3.19	202.5	96.5
			479.5	
$^{27}Al(n,\alpha)^{24}Na$	100	14.97	1368.5	100
			2754.4	99.9
$^{56}Fe(n,p)^{46}Mn$	91.7	2.58	846.6	98.9
			1810.7	27.2

Table 3
Decay data for the radio-nuclides used in the evaluation.

could be measured with an ammeter. The neutron energy was checked with a stilbene neutron spectrometer which was placed 1 m behind the fission chamber. A schematic diagram of these devices is shown in Figure 2.

The parameters for the irradiations are listed in Table 2. At the end of each irradiation, we began to measure the activity of the foils with two different semiconductor gamma detectors. The monitor foils were measured by a GeLi detector and the gamma spectra of the Zr foils were taken with a HPGe detector. Both devices were surrounded by lead shields with thick walls. The pulses from the detectors were collected with a 8192 channel analyzer card of an IBM AT computer. The random pile-up correction was determined using a pulse generator of known frequency.

Several spectra were recorded for each foil during the 'cooling time' interval of 7 minutes to 100 hours. From time-to-time, we analyzed the spectrum of ^{226}Ra for absolute determinations of the full energy peak and the total efficiency of the gamma spectra. This program[3] found the peaks automatically and performed peak shape and energy calibration on the basis of calibrations spectra. The peak area was calculated in two different ways: 1) the pulse counts of the peak channels were summed; 2) a

Energy of neutron	Cross section in mb
5.38±0.18	0.044±0.009
5.89±0.18	0.145±0.008
6.39±0.18	0.36±0.10
6.80±0.18	0.58±0.14
8.02±0.09	1.75±0.04
8.43±0.09	1.90±0.04
8.92±0.17	2.50±0.03
9.43±0.09	2.78±0.06
10.23±0.09	3.86±0.50
10.95±0.09	5.41±0.07
11.56±0.09	5.62±0.08
12.25±0.10	9.08±0.10

Table 4
Measured cross sections for the $^{90}Zr(n,p)^{90m}Y$ reaction.

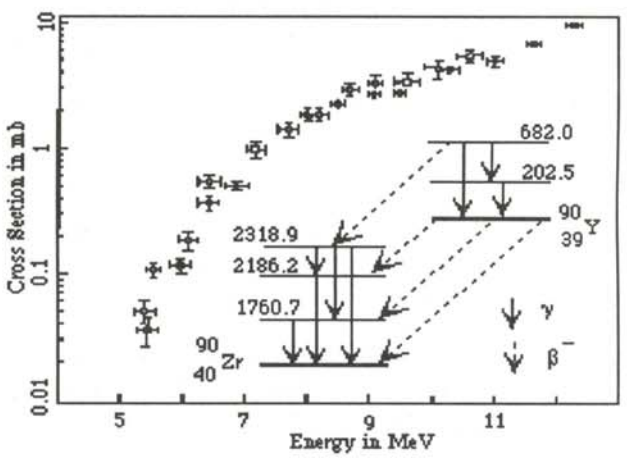

Figure 3
Measured cross section for the $^{90}Zr(n,p)^{90m}Y$ reaction. The solid symbols are our data, the open symbols data from Majah and Quaim.[8]

function was fit to the peak and the integral of this function determined. The final value given by the program was the average of these two values.

The decay curves for the different gamma lines were fitted using the method of least squares. The decay data for the reactions of the foils are listed in Table 3. The initial (extrapolated) activity was calculated from this decay curve. This activity was corrected for the cascade coincidence losses and for the self-absorption of the foils. The necessary data for these corrections were taken the literature [4,5,6]. The correction [7] for deuteron energies higher than 4.5 MeV (because of the $^2H(d,n\,p)^2H$ reaction) was determined on the basis of the literature.

RESULTS AND DISCUSSION

The cross section results are listed in Table 4 and shown in Figure 3. The results of Majah and Quaim[8] are also represented in Figure 3. The neutron flux densities were determined using the Al and Fe monitor foils. The errors in the cross sections shown in Figure 3 and Table 4 are the statistical uncertainties of the activity only.

If we compare the two experiments shown in Figure 3, we observe that our results are systematically lower than those of Majah and Quaim. This may be because we used other literature data for the monitor reactions and we used a different correction method. However, the results are still in reasonable agreement. Our three highest energy points are the first measurements in the 10.5 MeV - 12.3 MeV range.

ACKNOWLEDGMENTS

The author would like to thank Dr. Peter Raics for his help and support. He also wishes to thank Professor László Baksay for his advice.

REFERENCES

1. Kossuth Lajos University, Debrecen, Hungary.

2. The cyclotron is running at the Nuclear Research Institute of the Hungarian Academy of Sciences, Debrecen, Hungary.

3. S. Nagy, GAMANAL XT/AT User's Manual, Institute of Experimental Physics, KLTE Version 1.1, December 1989, (unpublished).

4. U. Reus and W. Westmeier, "Catalog of Gamma Rays from Radioactive Decay: Parts I and II ", Atomic Data and Nucl. Data, Tables 29, 1 and 194 , 1983.

5. C.M. Lederer and V.S. Shirley, Editors, Table of Isotopes, 7th Ed., John Wiley and Sons, Inc., 1978.

6. E. Storm and H.J. Israel, Nucl. Data Tables., A7, 1970, p. 565.

7. We wanted to take the background from the different scattering processes into account by measuring with an air-gas target, but the results which were given by this method were not accurate.

8. M. Ibn Majah and S.M. Qaim, Nucl. Sci. Eng., 104, 1990, p. 271.

FACULTY SPONSOR

Dr. Peter Raics
Kossuth Lajos Tudományegyetem (KLTE)
Experimental Physics Department
P.F. 105
Debrecen 4001, Hungary

TRAINING NEURAL NETWORKS TO DISCRIMINATE SIGNALS FROM BACKGROUND NOISE

Dena McCown*
Duke University
Durham NC 27708-0305
received December 12, 1992

ABSTRACT

One of the major challenges in experimental high energy physics is to discover resonances of rare particles against a noisy background. To asses the suitability of neural networks for this task, we studied several simple configurations of signal and noise in a two-dimensional parameter space. The ability of the network to discriminate the signal depended sensitively on the configuration and can be greatly enhanced by suitable processing.

INTRODUCTION

The aim of many experiments in high energy physics is to discover and investigate the properties of rare particle. Often it is very difficult to discover the signature of these particles against the background. There are various techniques that are used to suppress the background, and thus enhance the relative signal strength, but none of the techniques currently used are optimal. Recently, it has been suggested that neural networks may be used very effectively for this task. [1]

It is still unclear, however, whether neural networks can perform an unbiased data analysis or whether they produce artificial signals due to information acquired during the training process. The objective of this project is to investigate this problem. We studied how a possible training bias can be avoided in some simplified models with two parameters where a complete solution is known. The results of this project will be used to identify the decay of unstable particles in a six-dimensional parameter space from background events.

NEURAL NETWORKS

A neural network is a computer program that simulates brain functions. Starting with the input, the program transfers information to various points in successive layers or levels of the program called hidden layers. Synaptic weights, multiplicative factors that designate how strongly information should be passed from one layer to the next, are determined by the network for each unit, or data locations within the layer. In the training process, the network takes the input, a specific training pattern in this case, and carries it through the network, assigning synaptic weights as it goes. Certain channels for data transfer from layer to layer are strengthened, and the network learns to use these channels. The output indicates which channels developed to be stronger than others. Using a known input and comparing the output will show whether or not the network developed the proper channels, thereby learning the pattern.

This network used has two inputs, one hidden or intermediate layer, ten units in each layer (as shown in figure 1) and 1 output. The program we used [2] could be expanded to any number of layers. Figure 2 shows the two-layered structure used later in the analysis. Each unit in each layer has several connections going into it. These connections have strengths or synaptic weights associated with them. Each individual unit value is multiplied by its synaptic weight and passed on to the next unit. This next unit then sums all of the weighted input values it is given. If that sum is greater than a specified threshold for that unit, the unit will 'fire', it will become active and proceed with passing its value to the next unit. The training phase of the network used here utilizes error back propagation. The desired output is compared with the actual output and that information is sent back through the network so that the synaptic weights can be adjusted. The process is then repeated.

Dena received her B.Sc. in physics from Duke University in May, 1992. She did this research as part of the Undergraduate Research Support program at Duke during the 1991-92 academic year. She is currently pursuing an M.S. in medical physics at M.D. Anderson Cancer Center.

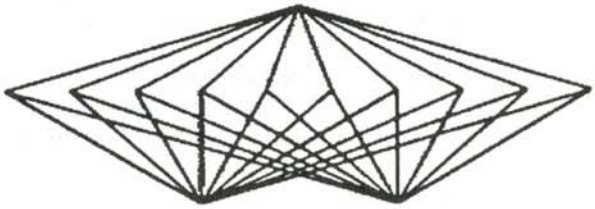

Figure 1
Schematic diagram of a one-layered network.

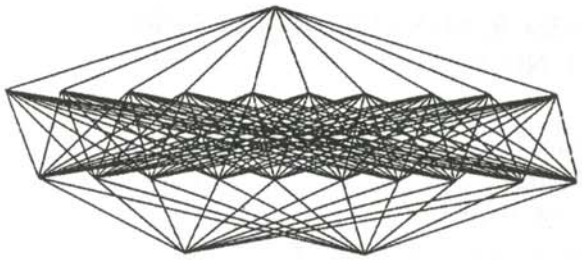

Figure 2
Connectivity structure of a two-layered network.

THE PROJECT

To begin this phase of the project, we decided to test some very simple structures. Using MATHEMATICA™ [3], we generated programs for several data sets with half of the data coded as signal (target output value of 1) and half as background (target output value of 0). We chose the geometries shown in Figure 3: a) a two-sided rectangle and a foursquare; b) two concentric circles; and b) a rectangle overlaid with a ring, where the rectangle is coded as background and the ring is coded as signal. The first two patterns have the same geometrical structure, but one is coded as four separate squares with signal and background arranged in a chessboard-like pattern. The other is coded as two vertical rectangles, one left and one right of the y-axis. Random assignments for coding were used as often as possible. These data were then fed into the network and analyzed to see if and how the network was working. A working network would successfully separate signals from background.

The network program was run on a NeXT™ computer. The random functions used for initialization did not function properly on the NeXT™ system, so a new one had to be added. Various stages of output were printed to monitor the network's function: errors for each data point were printed and the convergence patterns monitored. The synaptic weights were corrected by the new random number generator. When all the 'bugs' were out of the program, the network could distinguish between a signal and a background in the simple models: a two-sided rectangle and the foursquare.

The performance was fairly good. For the simple models, almost every point converged to a one or zero. As the models got more complicated the convergence was less perfect, but still good. All data samples were run with 100 data points and 100-500 iterations. The simpler the data set, the fewer iterations were needed for convergence.

The next stage was to try the rectangle/ring. Some trouble arose because of the overlap between the signal and the background. The network needed more hidden layers to distinguish this model. To verify this network need, the program was run with one layer for 500 iterations. The results were not good. The network seemed to move to 0.5 frequently, indicating that it could not discriminate between signal and background. Two layers did not produce significantly better results after 500 iterations.

GENERATING GRAPHICAL OUTPUT

To convert the output of the neural network program from column form to graphical form, and thereby verify that the network was learning the appropriate picture, MATHLINK™ [4] was used to connect the C-program simulating the neural network to MATHEMATICA™. Several minor changes had to be made to the C-program so that it would interface with MATHEMATICA™ and MATHLINK™. A template file was also established to serve as a 'decoder' for the connection. Once the link was established, MATHEMATICA™ was directed to plot a certain area of a coordinate system with the results of the network calculations. The parameters for plotting varied depending on the area in which the pattern was located. MATHEMATICA™ would then take each point in that specific area and give that point as input to the network. The network would give the number it had learned for that point (something between 1 and 0). Finally, MATHEMATICA™ would plot all three coordinates, the two that designate a point in the area and the network's output for that point, in a 3-D plot. The plots were to imitate the design the network was to learn.

The network did learn the pattern of the two-sided rectangle. The results are shown in Figure 4a. The optimum network structure was two hidden layers with 20 units each. The foursquare picture was more complicated for the network to learn. The same network structures proved to be optimal for the four square as were for the rectangle. However, the network did not learn to raise the appropriate points in the lower section of the graph. The best results obtained are shown in Figure 4b. Since the network did learn the first pattern, but could not learn the second, we determined that the foursquare violated some fundamental principle and a general form of the network will not be able to learn this pattern. Perhaps a more elaborate network or one specifically programmed to learn this pattern world perform the task better.

The best results for the rectangle and circle pattern with overlapping signal and background points was obtained with 200 training patterns, 20 units per layer and 2 hidden layers shown in the upper middle graph in Figure 5.

We began testing the hypothesis that the network would learn circular pattern better when trained with polar

(a) *(b)*

Figure 3
The geometry used as training patterns.

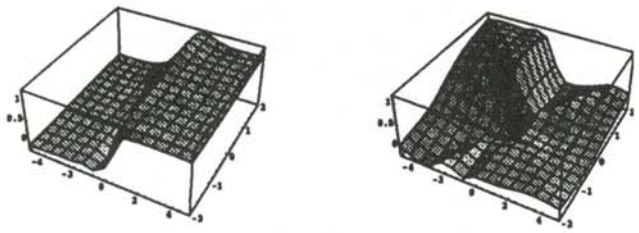

(a) (b)

Figure 4
Patterns the network learned for the: a) two-sided rectangle and b) four-square training patterns.

coordinates. The same points were generated by MATHEMATICA™ and stored in two separate files, one in rectangular coordinates and one in polar coordinates. The network was then trained on each so that a comparison could be made. After several tries with the polar data, the network was consistently producing very large error values, initially leading to the conclusion that the network could not train in polar coordinates. However, once the limits were changed for the units per layer, the network did respond properly. Fairly good results were obtained for the configuration with polar coordinates (shown in the top right of Figure 5), but preliminary finding indicated that the network was not capable of distinguishing the overlap well.

The assumption that we made was that the network could learn patterns that had few and very definite breaks which the overlap could not provide. To check this, the configuration was slightly altered so that the rectangle became a square, completely enclosed by the ring (lower left Figure 5). The results for the rectangular coordinates (bottom middle of Figure 5) were not any better, but the polar results (bottom left of Figure 5) showed significant improvements. This lead us to the conclusion that a suitable preprocessor was needed for the data before feeding it to the network. In this case, the preprocessor simply translated the data from rectangular to polar coordinates. The exact function of the preprocessor will depend upon the training pattern and the specific form in

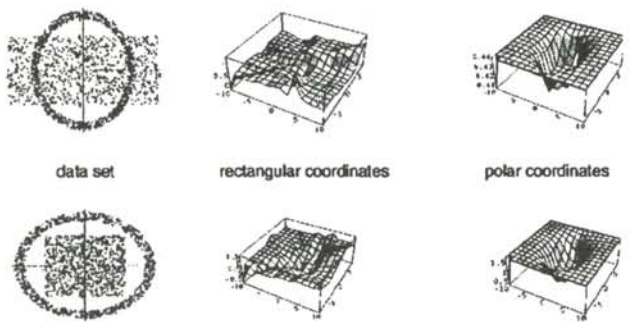

Figure 5
Data sets used and patterns learned for rectangular and polar coordinates.

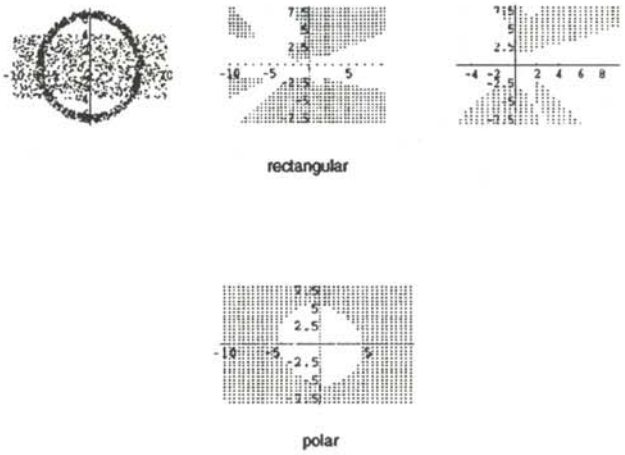

Figure 6
Data sets and results for network learned values above 0.5 and 0.7 (rectangular training) and above 0.43 (polar training).

which the network requires its input.

In the next phase of the evaluation, MATHEMATICA™ was asked to plot all x and y points for which the network attained higher than a particular value. Here we expected the configuration to improve as the cutoff value for the graph increased. The top part of Figure 6 shows the results for the overlapping configuration trained in rectangular coordinates. The middle graph is plotted for points above 0.5 and the right graph for points above 0.7. The lower part of Figure 6 plots the same data set trained in polar coordinates for network values above 0.43. The polar training was more effective in obtaining the desired shape, but not for obtaining the desired values. The network did not assign any values higher than 0.44 for this pattern.

The same analysis was performed for the configuration of the rectangle completely inside of the ring, with better results. Figure 7a shows the data set; Figure 7b shows the training in rectangular coordinates and plotted when the network attained a value of 0.5; Figure 7c the graph of the points for which the network learned greater than 0.5 when trained in polar coordinates and Figure 7d, for polar coordinates for which the network learned a value greater than 0.7.

SUMMARY

Several facts about a neural network have been learned. First, there is an optimal network configuration for each different data set that the network is to learn; that is, more complicated training patterns require more hidden layers. Second, a preprocessor is needed before feeding the data to the network. Finally, the network will train better when the signal and the background points do not overlap. All of this should be valuable insights when attempting to apply neural networks to data analysis in high-energy physics.

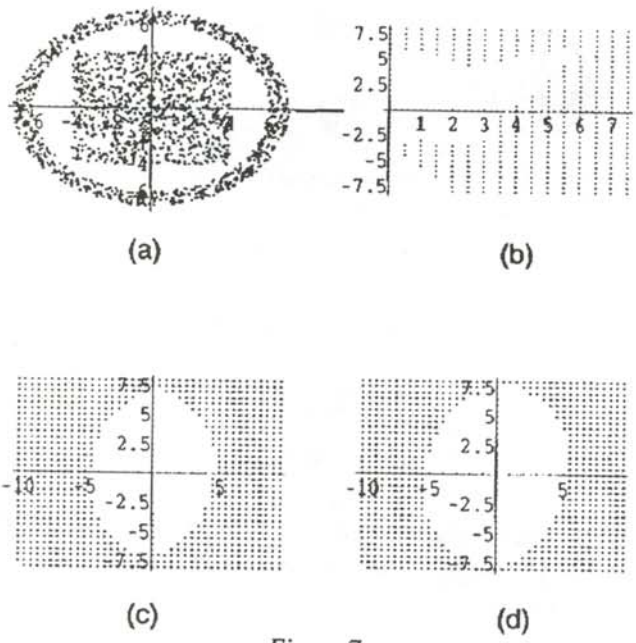

Figure 7

a) Data set used to obtain network values b) greater than 0.5 for rectangular coordinates; c) greater than 0.5 and d) greater than 0.7 for polar coordinates.

ACKNOWLEDGMENTS

This research was sponsored by Professor Berndt Müller in the Physics Department at Duke University. The author wants to thank Jochen Rau for assistance during the course of this work. This work was supported in part by an undergraduate research grant from Duke University and by a grant from the U.S. Department of Energy (DE-FG05-90ER40592)

REFERENCES

* Current address of author: Radiation Physics, M.D. Anderson Cancer Center, Texas Medical Center, 1515 Holcombe Blvd., Houston, TX 77030.

1. C. Peterson, Neural Networks as Classifiers in Sub-atomic Physics, Nucl. Phys. News, 2, 1992, p. 24-18; B. Denby, The Use of Neural Networks in High-Energy Physics, preprint FERMILAB-PUB-92-215-E, August 1992; C. Bortolotto, et. al., Neural Networks in Experimental High-Energy Physics, Int. J. Mod. Phys., C3, 1992, pp. 733-771; L. Lonnbald, C. Peterson and T. Rognvaldsson, Pattern Recognition in High-Energy Physics with Artificial Neural Networks: JETNET 2.0, Comp. Phys. Comm., 70, 1992, pp. 167-182.

2. We used a modified version of the computer program PERFUNC.C, published in **Neural Networks-An Introduction**, B. Müller and J. Reinhardt, Springer-Verlag, Berlin, 1990.

3. S. Wolfram, MATHEMATICA: A System for Doing Mathematics by Computer, Addison-Wesley, Redwood City, 1988.

4. Mathlink Reference Guide, Wolfram Research, 1991-1992.

FACULTY SPONSOR

Dr. Berndt Müller
Department of Physics
Duke University
Durham, NC 27708-0305

THE ONE-DIMENSIONAL NON-HOMOGENEOUS WAVE EQUATION

Nedal Saleh *
Physics Department
Yarmouk University
Irbid, Jordan
received March 15, 1993

ABSTRACT

The well known ideal wave equation is valid only for homogeneous media, where the wave propagation speed must be constant. In this paper, a modification of the wave equation is made so that it describes a disturbance propagating in a non-homogenous medium. Two examples of this equation are worked out.

INTRODUCTION

The one-dimensional wave equation is:

$$\frac{\partial^2\psi}{\partial x^2} - \frac{1}{v^2}\frac{\partial^2\psi}{\partial t^2} = 0 \ , \qquad (1)$$

where v is a constant, the velocity of the wave. Solutions to Equation 1 describes any disturbance (wave) propagating in a homogeneous medium. However, if the medium is not homogenous, Equation 1 cannot be used to describe the motion of the wave. [1] The non-homogeneity is manifested in the velocity of the disturbance not being constant, but depending position.

DERIVATION

If $\psi = \psi(x,t)$ represents a one-dimensional disturbance or wave, we can write:

$$\frac{\partial\psi}{\partial t} = \frac{\partial\psi}{\partial x}\frac{\partial x}{\partial t} = \frac{\partial\psi}{\partial x}\,v \ , \qquad (2)$$

where v is the velocity of the disturbance. Differentiating Equation 2 with respect to the spatial coordinate x gives:

$$\frac{\partial^2\psi}{\partial x\,\partial t} = \frac{\partial^2\psi}{\partial x^2}\,v + \frac{\partial\psi}{\partial x}\frac{\partial v}{\partial x} \ . \qquad (3)$$

If the velocity v is assumed to be independent of time, differentiating Equation 2 with respect to time gives:

$$\frac{\partial^2\psi}{\partial t^2} = \frac{\partial^2\psi}{\partial x\,\partial t}\,v \ . \qquad (4)$$

Equating the mixed second derivative terms in Equations 3 and 4 gives:

$$\frac{\partial^2 y}{\partial x^2}\,v + \frac{\partial\psi}{\partial x}\frac{\partial v}{\partial x} = \frac{1}{v}\frac{\partial^2\psi}{\partial t^2} \ . \qquad (5)$$

Rearranging the terms in Equation 5 yields:

$$\frac{\partial^2 y}{\partial x^2} + \frac{1}{v}\frac{\partial\psi}{\partial x}\frac{\partial v}{\partial x} - \frac{1}{v^2}\frac{\partial^2\psi}{\partial t^2} = 0 \ . \qquad (6)$$

Equation 6 is the non-homogeneous wave equation in one dimension. Notice that when v is a constant, the middle term in Equation 6 vanishes and we obtain the ordinary wave equation (Equation 1) as a special case.

SOLUTIONS

It can be shown [2] by direct substitution that the general solution to Equation 6 has the form:

$$\psi(x,t) = G\left(x - \int_0^t v(t')\,dt'\right) + F\left(x + \int_0^t v(t')\,dt'\right) \ , \qquad (7)$$

where $v(t)$ is the velocity of the wave front as a function of time, and F and G are continuous functions having as their argument the term $x \pm \int v(t')\,dt'$.

One can also think of a solution to Equation 6 that is of the form:

$$\psi(x,t) = \chi(x)\,T(t) \ , \qquad (8)$$

where $\chi(x)$ is only a function of position, x, and $T(t)$ is only a function of time, t. Substituting Equation 8 into Equation 6 and separating the variables produces two ordinary differential equations:

$$\frac{d^2T}{dt^2} + \omega^2\,T = 0 \ , \qquad (9)$$

and

$$\frac{d^2\chi}{dx^2} + \frac{1}{v}\frac{dv}{dx}\frac{d\chi}{dx} + \frac{\omega^2}{v^2}\,\chi = 0 \ , \qquad (10)$$

where ω^2 is the separation constant. Equation 9 is the equation that describes the motion of a simple harmonic oscillator. Equation 10 is the one-dimensional time-independent wave equation for a non-homogeneous medium.

Equation 9 has a significant physical implication: the frequency of the wave in a non-homogeneous medium is

Nedal graduated from Yarmouk University, Jordan, during the summer of 1993. This paper came out of his interest in the foundations of quantum mechanics and re-formulation of quantum theory. Nedal is currently pursuing his Master's degree at Western Michigan University-Kalamazoo. He is worried about the recession in the job market for theoretical physicists.

constant, the effect of the inhomogeneity is reflected only upon the wavelength and the velocity.

EXAMPLES

A medium with varying index of refraction.

In an optically non-homogeneous medium, the refractive index in not constant throughout the medium, but could depend upon many variabales. For simplicity, we will assume a one-dimensional dependence of the refractive index:

$$v(x) = \frac{c}{n(x)} \quad and \quad \frac{dv}{dx} = -\frac{c}{n^2(x)}\frac{dn}{dx} \; . \tag{11}$$

Substituting Equations 11 into Equation 10 yields:

$$\frac{d^2\chi}{dx^2} - \frac{1}{n(x)}\frac{dn}{dx}\frac{d\chi}{dx} + \left[\frac{\omega\, n(x)}{c}\right]^2 \chi = 0 \; . \tag{12}$$

If we know how the index of refraction depends upon position, we can solve this linear differential equation for the space function $\chi(x)$.

The two independent solutions of Equation 12 take on the form:

$$\chi(x) = A \exp\left\{ i\frac{\omega}{c}\int_0^x n(x')\,dx' \right\} + B \exp\left\{ -i\frac{\omega}{c}\int_0^x n(x')\,dx' \right\}, \tag{13}$$

where A and B are arbitrary constants,

Mechanical (sound) waves in a medium of varying density

In a medium of varying density, the velocity of a propagating sound wave is related to the density of the medium as:

$$v^2(x) = \frac{B}{\rho(x)} \; , \tag{14}$$

where B is the bulk modulus of the medium and $\rho(x)$ is the density of the medium. We will assume that the bulk modulus is constant. For this situation, Equations 11 become:

$$v(x) = \sqrt{\frac{B}{\rho(x)}} \quad and \quad \frac{dv}{dx} = -\frac{1}{2}\sqrt{\frac{B}{\rho^3(x)}}\frac{d\rho(x)}{dx} \; . \tag{15}$$

Substituting Equations 15 into Equation 10 gives:

$$\frac{d^2\chi}{dx^2} + \frac{1}{2}\frac{1}{\rho(x)}\frac{d\rho(x)}{dx}\frac{d\chi}{dx} + \frac{\rho(x)\,\omega^2}{B}\chi = 0 \; . \tag{16}$$

In the same manner as before, the general solution to Equation 16 has the form:

$$\chi(x) = A \exp\left\{ i\frac{\omega}{\sqrt{B}}\int_0^x \sqrt{\rho(x')}\,dx' \right\} + B \exp\left\{ -i\frac{\omega}{\sqrt{B}}\int_0^x \sqrt{\rho(x')}\,dx' \right\} \tag{17}$$

where A and B are arbitrary constants.

Finally, in quantum theory, Equation 6 may be a modified version of the Schrödinger equation, with v, the velocity, representing the group velocity and ψ representing the motion of the expectation value.

ACKNOWLEDGMENTS

The author would like to thank Mr. Fuad Rawwagah and Dr. Sami Mahmoud for their assistance in preparing this manuscript.

REFERENCES

* Current address of the author: Physics Department, Western Michigan University, Kalamazoo, MI, 49008.

1. Many authors did not heed this point. See for example: S. Lipson, OPTICAL PHYSICS, Cambridge University Press, UK, 1969, p. 89; Zhu et.al. Am. J. Phys., 54, 7 July 1986, p. 604; and H. Goldstein, CLASSICAL MECHANICS, Addison Wesley, 2nd Edition, 1980, pp. 487-489.

2. The proof by direct substitution begins with Equation 7

$$\psi(x,t) = G\left(x - \int_0^t v(t')\,dt'\right) + F\left(x + \int_0^t v(t')\,dt'\right) \; ,$$

The second derivative with respect to position is:

$$\frac{\partial^2}{\partial x^2}\psi(x,t) = \frac{\partial^2 G}{\partial x^2} + \frac{\partial^2 F}{\partial x^2} \; .$$

The first derivataive with respect to time is:

$$\frac{\partial}{\partial t}\psi(x,t) = \frac{\partial G}{\partial u_-}(-v) + \frac{\partial F}{\partial u_+}(v) \; ,$$

$$\text{where } u_\pm = x \pm \int_0^t v(t')\,dt' \; .$$

Taking the second derivative gives:

$$\frac{\partial^2}{\partial t^2}\psi(x,t) = \frac{\partial^2 G}{\partial u_-^2}(-v)^2 + \frac{\partial G}{\partial u_-}\frac{\partial v}{\partial t} + \frac{\partial^2 F}{\partial u_-^2}(v)^2 + \frac{\partial F}{\partial u_+}\frac{\partial v}{\partial t} \; .$$

Using the fact that $\frac{\partial v}{\partial t} = \frac{\partial v}{\partial x}\frac{\partial x}{\partial t} = \frac{\partial v}{\partial x}\,v$,

Equation 6 becomes: $\left(\frac{\partial^2 G}{\partial x^2} - \frac{\partial^2 G}{\partial u_-^2}\right) + \left(\frac{\partial^2 F}{\partial x^2} - \frac{\partial^2 F}{\partial u_-^2}\right)$

$$+ \frac{1}{v}\frac{\partial v}{\partial x}\left[\left(\frac{\partial G}{\partial x} - \frac{\partial G}{\partial u_-}\right) + \left(\frac{\partial F}{\partial x} - \frac{\partial F}{\partial u_+}\right)\right].$$

The terms in the round brackets vanish because:

$$\frac{\partial}{\partial_\pm} = \frac{\partial x}{\partial u_\pm}\frac{\partial}{\partial x} = \frac{1}{\frac{\partial u_\pm}{\partial x}}\frac{\partial}{\partial x} = \frac{\partial}{\partial x}$$

thus showing that Equation 7 is a solution to Equation 6 by direct substitution.

FACULTY SPONSOR

Professor Nabil Ayoub, Chairman
Physics Department
Yarmouk University
Irbid 211-63 Jordan

Undergraduate Research - Making Physics Interesting to all Students.

An Editorial by Rexford E. Adelberger

When invited to parties outside of the college where I work, I don't look forward to someone who does not know me asking what I do for a living. When I say that I am a physicist, there is often an uncomfortable pause, and then the somewhat apologetic response that they are very interested in science, but it was not something that they 'did'. My neighbors and friends are really bright and very hard working, but for some reason, my studying physics seems to have made me different and slightly weird in the eyes of people who work in offices, industrial plants or own their own small businesses. In my own view, I am not really different; it is just that my passion is physics while theirs is balancing books, selling insurance or healing sick individuals. How, in the eyes of the nonacademic world, did physics become a thing that only a very few and somewhat special people can do. Why did I decide to study and 'do' physics rather than the things my neighbors did?

During my undergraduate years, the compulsory military draft helped a lot. I found that studying physics was much easier than getting drafted and having to fight on some foreign shore a war which I was not too sure that I believed was just. It wasn't physics as much as the very distressing alternatives that kept me going. The same might also be said for by decision to go on to graduate school: it seemed a much better thing to do than to have to work in a low paying job or killing people who I did not hate.

At some time during my graduate study, physics became the compelling factor rather than the alternatives. This metamorphosis occurred at the point where I stopped studying physics and started being a physicist. Being a physicist was was alluring to me as the beautiful song of the Lorelei was to the ancient boaters on the Rhine river. When I began to understand something about nature because of the experiments I designed, it was as if I were playing with the Gods. Wow!! I thought that I was really something special. Why did I wait so long to become a physicist?

Spending those countless late night hours working complex nasty thermodynamics problems and obscure seemingly irrelevant mechanics exercises would have been much more meaningful and reasonable if only I had been a physicist as well. Maybe the reason that all my neighbors stayed away from physics while they were in college is that they never had a chance to be a physicist, their only option was to study physics.

When I began my career at a teacher at the undergraduate level, this revelation remained with me, but somewhat buried by the reality of preparing lectures and making sure that the lab equipment was working properly. As I talked with my colleagues about my ideas, they reminded me that only the best students can do research. Students first had to prove themselves in the class room before they were invited into the research labs. If they 'passed the muster', they would work on the research projects that the faculty were doing to get tenure and promotions. This was real physics.

My insight into how to get young people interested in physics received a significant dose of 'fertilizer' when I went to teach in a small, low budget, high contact hour private liberal arts college. The dean told me if there were lots of physics majors at the college, then the budget and the number of faculty would be increased to reflect the number of students taking physics classes. I wondered if it would be possible to have lots of students as apprentice physicists rather than a few students taking advanced physics courses and lots of people taking 'physics for people who do not want to take physics but have to'.

My experience of the last 20 years is convincing experimental evidence that my early insight was indeed correct. All sorts of students are fascinated by being physicists. They come to our college study all sorts of things, but are drawn to the excitement shown in the science departments where young people are being scientists. What I did not expect to find out was that doing research plays a significant role in the retention and eventual success of the student who, in the traditional evaluations of physics students, would be labeled as a weak student. These young people often seem to flourish in the real scientific world and active participation in research gives them the confidence to do the more traditional parts of the physics curriculum.

The undergraduate research about which I am talking is a special pedagogical strategy. Research is not just a reward for the best students to do in their final year at the college using specialized expensive equipment, but a deliberate exercise that starts in the freshman year and is the common thread that binds together the full 4 years of the physics curriculum. This model was built on an idea presented to me by Dudley Herschbach, a Nobel Laureate who, among many other things, teaches undergraduate students at Harvard. He told me that learning about nature is really amazing. You can ask any sort of question to nature and it answers you correctly. It never tells you things that are not true. The problem we have is that we too often ask the wrong question of nature or that the question we asked

was not the one we thought we were asking. The difficult part is to listen to the answers that nature gives. As we cross examine nature and explore blind alleys, our colleagues commend us even though we do not have answers. Finally, when we ask sufficient and correct questions, and consequently discover something new about nature, the world applauds us.

Apparently nature want us to know how it operates. What we have to do with students is to teach them to ask questions and how to listen to the answers nature gives them. This is certainly a different mode of operation than teaching students a bunch of cold facts and asking them to solve a series of problems whose answers are in the back of the book. It requires the individual student to interact with nature and to form a model of what is happening in their own mind using the answers that nature has presented to them. The responsibility and excitement of learning belongs to the student!

It became clear to me that if you want first year undergraduate students to become physicists, you can't expect them do the kind of research that one does for a Ph.D. or for getting promotions and tenure. What the students have to learn is to read journals, design experiments and ask questions of nature. It amazes me how well written and easy to understand the papers are that were written at the turn of the century that appeared in journals such as Physical Review and Philosophical Magazine. They can be understood, with some help from the faculty, by most beginning students. These papers are better written than many of the text books that are currently on the book store shelves.

It becomes our responsiblity to show students how to model reality instead just working problems about the 'frictionless and horizontal railroad'. They have to be presented problems that do not have answers that can looked up somewhere to judge if it has been worked correctly. We have to provide a platform where the student can gain confidence in the way that they understand nature. This confidence can be achieved by presenting their work to their peers in the lab as well as regional meetings such as are sponsored by many SPS chapters. Being a community of learners is much more attractive than working problems in the quiet lonely surroundings of the library or a dorm room.

To start an undergraduate research program one doesn't need to get outside funding from the NSF or some prestigious private foundation. It is a matter of how we present physics to our students and how we use the computers and lab equipment that already exist in the schools where we teach.

Students must to be allowed to make and learn from their own mistakes. It amazes me how quickly you can turn off a student by telling them the answer to their questions rather than having them do an experiment and listen to nature's response to their question. When students become accustomed to hearing about and working with things that they do not completely understand, they are well on their way to becoming a practicing scientists. The role of the teacher in this system is to show the student to decide what are important questions, and how to listen to and evaluate the answers that nature gives. After all, there is no higher authority in physics than nature itself.

The Journal of Undergraduate Research in Physics

The Journal of Undergraduate Research in Physics is the journal of Sigma Pi Sigma and the Society of Physics Students. It is published by the Physics Department of Guilford College, Greensboro NC 27410. Inquiries about the journal should be sent to the editorial office.

The Journal of Undergraduate Research in Physics

Editorial Office -
The Journal of Undergraduate Research in Physics
Physics Department
Guilford College
Greensboro, NC 27410
910-316-2279 (voice)
910-316-2951 (FAX)

Editor -
Dr. Rexford E. Adelberger
Professor of Physics
Physics Department
Guilford College
Greensboro, NC 27410
ADELBERGERRE@RASCAL.GUILFORD.EDU

The Society of Physics Students

National Office -
Dr. Donald Kirwin, Executive Director
Ms. Sonja Lopez, SPS Supervisor
Society of Physics Students
American Institute of Physics
1 Physics Ellipse
College Park, MD 20740
301-209-3007

President of the Society -
Dr. Fred Domann
Department of Physics
University of Wisconsin at Platteville

President of Sigma Pi Sigma -
Dr. Reuben James
Department of Physics
SUNY College at Oneonta